Numerical modeling of neutron transport in SP$_3$ approximation by finite element method

Alexander V. Avvakumov[a], Valery F. Strizhov[b], Petr N. Vabishchevich[b,c,*], Alexander O. Vasilev[c]

[a]National Research Center Kurchatov Institute, 1, Sq. Academician Kurchatov, Moscow, Russia
[b]Nuclear Safety Institute, Russian Academy of Sciences, 52, B. Tulskaya, Moscow, Russia
[c]North-Eastern Federal University, 58, Belinskogo, Yakutsk, Russia

Abstract

The SP$_3$ approximation of the neutron transport equation allows improving the accuracy for both static and transient simulations for reactor core analysis compared with the neutron diffusion theory. Besides, the SP$_3$ calculation costs are much less than higher order transport methods (S$_N$ or P$_N$). Another advantage of the SP$_3$ approximation is a similar structure of equations that is used in the diffusion method. Therefore, there is no difficulty to implement the SP$_3$ solution option to the multi-group neutron diffusion codes. In this work, the application of the SP$_3$ methodology based on solution of the λ- and α-spectral problems has been tested for the IAEA-2D and HWR reactor benchmark tests. The FEM is chosen to achieve the 3D geometrical generality, using GMSH as a generic mesh generator. The results calculated with the diffusion and SP$_3$ methods are compared with the reference transport calculation results. It was found for the HWR reactor test that some eigenvalues are complex when calculating using both diffusion and SP$_3$ options.

Keywords: neutron transport equation, diffusion theory, SP$_3$ approximation, reactor core, spectral problems, eigenvalues.

1. Introduction

The diffusion approximation of the neutron transport equation is widely used in nuclear reactor analysis allowing whole-core calculations with reasonable accuracy. The main feature of neutron diffusion equation is following: it is assumed that the neutron current is proportional to the neutron flux gradient (the Ficks law). There are also three assumptions: neutron absorption much less

---

*Corresponding author

Email addresses: `Avvakumov2009@rambler.ru` (Alexander V. Avvakumov), `vfs@ibrae.ac.ru` (Valery F. Strizhov), `vabishchevich@gmail.com` (Petr N. Vabishchevich), `haska87@gmail.com` (Alexander O. Vasilev)

likely than scattering, linear spatial variation of the neutron distribution and isotropic scattering (Stacey, 2007). To provide the validity of diffusion theory, the modern diffusion codes use, as a rule, assembly-by-assembly coarse-mesh calculation scheme with effective homogenized cross sections, prepared by more accurate transport approximations. To improve the diffusion code restrictions related with limitations on mesh spacing, different approaches are used including nodal and finite element methods (Avvakumov et al., 2017; Lawrence, 1986).

For many situations of interest (for instance, the pin-by-pin calculation taking account strongly absorbing control rods), the applicability of neutron diffusion theory are limited. Therefore, a more rigorous approximation for the neutron transport is required.

The solution of the neutron transport equation is very complicated problem because of seven independent variables: five for space-angular description, one for energy and one for time. To simplify the transport problem, different approaches are used such as the spherical harmonics (P_N) approximation (Azmy and Sartori, 2010). The P_N approximation of the neutron transport equation is derived by expansion of the angular dependence of the neutron flux in the N spherical harmonics. During the last time, the simplest version of the P_N method, namely the simplified P_N approximation became widespread (McClarren, 2010). The major feature of the SP_N method is following: the three-dimensional neutron transport equation is transformed to a set of one-dimensional equations. The number of the SP_N trial functions is equal to $2(N+1)$ compared with the P_N method which uses $(N+1)^2$ trial functions. This leads to significant reduce in the computation time for typical whole-core calculations.

The SP_N approximation was first derived by Gelbard (Gelbard, 1960, 1961, 1962) in the early 1960s. He replaced the spatial derivatives with Laplacian and divergence operators in a one-dimensional planar geometry. The resulting SP_N equations are elliptic, for example, the SP_3 equations consist of two equations of diffusion type with two unknown fluxes: the scalar flux and the second angular flux moment. More rigorous theoretical foundation of the SP_3 methodology has been derived by Brantley and Larsen (Brantley and Larsen, 2000) on the basis of variational methods.

The SP_3 method, as expected, can provide accuracy improvement compared with the common used diffusion method. Besides, implementation of the SP_3 equations into the diffusion code is not difficult because of the similar structure of the SP_3 and diffusion equations. For this reason the SP_3 method was adopted in different whole-core calculation codes, such as DYN3D (Beckert and Grundmann, 2008), PARCS (Downar et al., 2010) and others. According to (Tada et al., 2008), application of the SP_3 theory to the pin-by-pin calculation for BWR geometry resulted in remarkable improvement in the calculation accuracy compared with the diffusion method. Besides, as it turned out, the computation time using the SP_3 method is only 1.5 times longer than that using the diffusion method (Tada et al., 2008).

Thus, the SP_3 method can be considered as an improved approximation of the neutron transport equation compared with the diffusion method. In this

regard, it will be very useful to compare the spectral parameters, calculated by both the diffusion and SP$_3$ methods. To characterize the reactor steady-state conditions or dynamic behavior, some spectral problems are considered (Stacey, 2007; Bell and Glasstone, 1970). The steady-state condition is usually described by solution of a spectral problem (λ-eigenvalue problem); the fundamental eigenvalue (the largest eigenvalue) is called k-effective of the reactor core (Stacey, 2007; Bell and Glasstone, 1970). The reactor dynamic behavior can naturally be described on the basis of the approximate solution expansion in time-eigenvalue of α-eigenvalue problem (Ginestar et al., 2002; Verdu et al., 2010; Verdú and Ginestar, 2014). At large times, one can talk about the asymptotic behavior of a neutron flux, whose amplitude is $\exp(\alpha t)$. Previously the complex eigenvalues and eigenfunctions were found in the spectral problems for some numerical tests (Avvakumov et al., 2017).

In this paper we consider the SP$_N$ approximation for the steady-state multigroup neutron transport problem. To solve spectral problems with nonsymmetrical matrices we use well-designed algorithms and relevant free software including the library SLEPc (Scalable Library for Eigenvalue Problem Computations, http://slepc.upv.es/). We use a Krylov-Schur algorithm, a variation of Arnoldi method, described in (Stewart, 2001).

The paper is organized as follows. The steady-state and dynamic models of a nuclear reactor based on the multigroup SP$_3$ equations are given in Section 2. In Section 3 we discuss various spectral problems. Some numerical examples of calculation of spectral characteristics of two-dimensional test problems for IAEA-2D benchmark problem and HWR reactor using the two-group system of diffusion and SP$_3$ equations is discussed in Section 4. The results of the work are summarized in Section 5.

2. Problem statement

Lets consider the symmetric form of the SP$_3$ equation for the neutron flux (Ryu and Joo, 2010). The neutron dynamics is considered in the limited convex two-dimensional or three-dimensional area Ω ($\boldsymbol{x} = \{x_1, ..., x_d\} \in \Omega, \ d = 2, 3$) with boundary $\partial\Omega$. The neutron transport is described by the system of equations

$$
\begin{aligned}
\frac{1}{v_g}\frac{\partial \phi_{0,g}}{\partial t} - \frac{2}{v_g}\frac{\partial \phi_{2,g}}{\partial t} &- \nabla \cdot D_{0,g}\nabla \phi_{0,g} + \Sigma_{r,g}\phi_{0,g} - 2\Sigma_{r,g}\phi_{2,g} = \\
&= (1-\beta)\chi_{n,g}S_n + S_{s,g} + \chi_{d,g}S_d, \\
-\frac{2}{v_g}\frac{\partial \phi_{0,g}}{\partial t} + \frac{9}{v_g}\frac{\partial \phi_{2,g}}{\partial t} &- \nabla \cdot D_{2,g}\nabla \phi_{2,g} + (5\Sigma_{t,g} + 4\Sigma_{r,g})\phi_{2,g} - 2\Sigma_{r,g}\phi_{0,g} = \\
&= -2(1-\beta)\chi_{n,g}S_n - 2S_{s,g} - 2\chi_{d,g}S_d,
\end{aligned}
\tag{1}
$$

where

$$
S_n = \sum_{g'=1}^{G} \nu\Sigma_{f,g'}\phi_{g'}, \quad S_{s,g} = \sum_{g\neq g'=1}^{G} \Sigma_{s,g'\to g}\phi_{g'}, \quad S_d = \sum_{m=1}^{M} \lambda_m c_m,
$$

3

$$\phi_{0,g} = \phi_g + 2\phi_{2,g}, \quad D_{0,g} = \frac{1}{3\Sigma_{tr,g}}, \quad D_{2,g} = \frac{9}{7\Sigma_{t,g}}, \quad g = 1, 2, ..., G.$$

Here G — number of energy groups, $\phi_g(\boldsymbol{x}, t)$ — scalar flux, $\phi_{0,g}(\boldsymbol{x}, t)$ — pseudo 0th moment of angular flux, $\phi_{2,g}(\boldsymbol{x}, t)$ — second moment of angular flux, $\Sigma_{t,g}(\boldsymbol{x}, t)$ — total cross-section, $\Sigma_{tr,g}(\boldsymbol{x}, t)$ — transport cross-section, $\Sigma_{r,g}(\boldsymbol{x}, t)$ — removal cross-section, $\Sigma_{s,g' \to g}(\boldsymbol{x}, t)$ — scattering cross-section, χ_g — spectra of neutrons, $\nu\Sigma_{f,g}(\boldsymbol{x}, t)$ — generation cross-section, $c_m(\boldsymbol{x}, t)$ — density of sources of delayed neutrons, λ_m — decay constant of sources of delayed neutrons, M — number of types of delayed neutrons.

The density of sources of delayed neutrons is described by the equations

$$\frac{\partial c_m}{\partial t} + \lambda_m c_m = \beta_m S_n, \quad m = 1, 2, ..., M, \tag{2}$$

where β_m is a fraction of delayed neutrons of m-type, and

$$\beta = \sum_{m=1}^{M} \beta_m.$$

The Marshak-type conditions are set at the boundary of the area $\partial\Omega$

$$\begin{bmatrix} J_{0,g}(\boldsymbol{x}) \\ J_{2,g}(\boldsymbol{x}) \end{bmatrix} = \begin{bmatrix} \dfrac{1}{2} & -\dfrac{3}{8} \\ -\dfrac{3}{8} & \dfrac{21}{8} \end{bmatrix} \begin{bmatrix} \phi_{0,g}(\boldsymbol{x}) \\ \phi_{2,g}(\boldsymbol{x}) \end{bmatrix}, \quad J_{i,g}(\boldsymbol{x}) = -D_{i,g}\nabla\phi_{i,g}(\boldsymbol{x}), \quad i = 0, 2. \tag{3}$$

System of equations (1) and (2) is supplemented with boundary conditions (3) and corresponding initial conditions

$$\phi_g(\boldsymbol{x}, 0) = \phi_g^0(\boldsymbol{x}), \quad g = 1, 2, ..., G, \quad c_m(\boldsymbol{x}, 0) = c_m^0(\boldsymbol{x}), \quad m = 1, 2, ..., M. \tag{4}$$

Let's write the boundary problem (1)–(4) in operator form. The vectors $\boldsymbol{u}_1 = \{\phi_{0,1}, \phi_{0,2}, \cdots, \phi_{0,G}\}$, $\boldsymbol{u}_2 = \{\phi_{2,1}, \phi_{2,2}, \cdots, \phi_{2,G}\}$, $\boldsymbol{c} = \{c_1, c_2, ..., c_M\}$ and matrices are defined as follows

$$V = (\mathrm{v}_{gg'}), \quad \mathrm{v}_{gg'} = \frac{1}{v_g}\delta_{gg'}, \quad B = (b_{gg'}), \quad b_{gg} = -2\Sigma_{r,g}, \quad b_{gg'} = 2\Sigma_{s,g' \to g},$$

$$A_1 = (a_{gg'}), \quad a_{gg} = -\nabla \cdot D_{0,g}\nabla + \Sigma_{r,g}, \quad a_{gg'} = -\Sigma_{s,g' \to g},$$

$$A_2 = (a_{gg'}), \quad a_{gg} = -\nabla \cdot D_{2,g}\nabla + 5\Sigma_{tr,g} + 4\Sigma_{r,g}, \quad a_{gg'} = -4\Sigma_{s,g' \to g},$$

$$F = (f_{gg'}), \quad f_{gg'} = \chi_{n,g}\nu\Sigma_{f,g'}, \quad E = (e_{gm}), \quad e_{gm} = \chi_{d,g}\lambda_m,$$

$$\Lambda = (\lambda_{mm'}), \quad \lambda_{mm'} = \delta_{mm'}\lambda_m, \quad Q = (q_{mg}), \quad q_{mg} = \beta_m\nu\Sigma_{f,g},$$

where

$$\delta_{gg'} = \begin{cases} 1, & g = g', \\ 0, & g \neq g', \end{cases}$$

is the Kronecker symbol. We shall use the set of vectors $\boldsymbol{u}$, whose components satisfy the boundary conditions (3). Using the set definitions, the system of equations (1) and (2) can be written as following

$$V(\frac{\partial \boldsymbol{u_1}}{\partial t} - 2\frac{\partial \boldsymbol{u_2}}{\partial t}) + A_1\boldsymbol{u_1} + B\boldsymbol{u_2} = (1-\beta)F(\boldsymbol{u_1} - 2\boldsymbol{u_2}) + E\boldsymbol{c},$$

$$V(-2\frac{\partial \boldsymbol{u_1}}{\partial t} + 9\frac{\partial \boldsymbol{u_2}}{\partial t}) + A_2\boldsymbol{u_2} + B\boldsymbol{u_1} = -2(1-\beta)F(\boldsymbol{u_1} - 2\boldsymbol{u_2}) - 2E\boldsymbol{c}, \qquad (5)$$

$$\frac{\partial \boldsymbol{c}}{dt} + \Lambda\boldsymbol{c} = Q(\boldsymbol{u_1} - 2\boldsymbol{u_2}).$$

Without delayed neutrons, we have

$$V(\frac{\partial \boldsymbol{u_1}}{\partial t} - 2\frac{\partial \boldsymbol{u_2}}{\partial t}) + A_1\boldsymbol{u_1} + B\boldsymbol{u_2} = F(\boldsymbol{u_1} - 2\boldsymbol{u_2}),$$

$$\qquad\qquad (6)$$

$$V(-2\frac{\partial \boldsymbol{u_1}}{\partial t} + 9\frac{\partial \boldsymbol{u_2}}{\partial t}) + A_2\boldsymbol{u_2} + B\boldsymbol{u_1} = -2F(\boldsymbol{u_1} - 2\boldsymbol{u_2}).$$

The Cauchy problem is formulated for equations (5) and (6) when

$$\boldsymbol{u_1}(0) = \boldsymbol{u_1^0}, \quad \boldsymbol{u_2}(0) = \boldsymbol{u_2^0}, \quad \boldsymbol{c}(0) = \boldsymbol{c^0}, \qquad (7)$$

where $\boldsymbol{u_1^0} = \{\phi_{0,1}^0, \phi_{0,2}^0, ..., \phi_{0,G}^0\}$, $\boldsymbol{u_2^0} = \{\phi_{2,1}^0, \phi_{2,2}^0, ..., \phi_{2,G}^0\}$ and $\boldsymbol{c^0} = \{c_1^0, c_2^0, ..., c_M^0\}$.

3. Spectral problems

To characterize the reactor dynamic processes described by Cauchy problem (5)-(7), lets consider some spectral problems (Bell and Glasstone, 1970; Stacey, 2007).

The spectral problem, which is known as the λ-spectral problem, is usually considered. For the system of equations (6), (7) without delayed neutrons, we have

$$L\boldsymbol{\varphi} = \lambda^{(k)}M\boldsymbol{\varphi}, \qquad (8)$$

where

$$\boldsymbol{\varphi} = \{\boldsymbol{\varphi_1}, \boldsymbol{\varphi_2}\}, \quad L = \begin{pmatrix} A_1 & B \\ B & A_2 \end{pmatrix}, \quad M = \begin{pmatrix} F & -2F \\ -2F & 4F \end{pmatrix}.$$

The minimal eigenvalue is used for characterisation of neutron field, thus

$$k = \frac{1}{\lambda_1^{(k)}}$$

is the effective multiplication factor (k-effective). The value $k = \lambda_1^{(k)} = 1$ is related to the critical state of the reactor, and the corresponding eigenfunction $\boldsymbol{\varphi}^{(1)}(\boldsymbol{x})$ is the stationary solution of the Eq (5), (6). At $k > 1$, one can speak about supercriticality, at $k < 1$ — about subcriticality.

The spectral problem (8) cannot directly be connected with the dynamic processes in a nuclear reactor. The eigenvalues of the multiplication factor of

5

the reactor and the corresponding eigenfunctions do not depend on the time delay for the emission of delayed neutrons. The reason is that the problem (8) on eigenvalues is the problem of finding time-independent solutions of the neutron transport equation, and the term describing the contribution of fission to the neutron balance is equal to the total number of fission neutrons, both instantaneous and delayed divided by k. At the best, we can get only the limiting case — the stationary critical state. The more acceptable spectral characteristics for the non-stationary equation (5) are related the spectral problem

$$L\boldsymbol{\varphi} - (1 - \beta)M\boldsymbol{\varphi} - I\boldsymbol{s} = \lambda^{(\alpha)}W\boldsymbol{\varphi},$$
$$\Lambda\boldsymbol{s} - R\boldsymbol{\varphi} = \lambda^{(\alpha)}\boldsymbol{s}. \tag{9}$$

Without delayed neutrons (6), we have

$$L\boldsymbol{\varphi} - M\boldsymbol{\varphi} = \lambda^{(\alpha)}W\boldsymbol{\varphi}, \tag{10}$$

where
$$I = \begin{pmatrix} E \\ -2E \end{pmatrix}, \quad R = \begin{pmatrix} Q & -2Q \end{pmatrix}, \quad W = \begin{pmatrix} V & -2V \\ -2V & 9V \end{pmatrix}$$

The fundamental eigenvalue
$$\alpha = \lambda_1^{(\alpha)}$$

is called (Bell and Glasstone, 1970) α-eigenvalues or period eigenvalues, because they are inversely related to the reactor periods. The problem of the period eigenvalues essentially takes into account the contribution of delayed neutrons. In particular, the long lifetime of the predecessors of delayed neutrons makes a large contribution to the slowly decreasing eigenfunctions of the reactor period, and this does not occur when only instantaneous neutrons are taken into account.

The asymptotic behaviour of Cauchy problem solution (5)-(7) at large times can be connected with the eigenvalue α. In this regular mode, the reactor behaviour is described by the function $\exp(-\alpha t)\boldsymbol{\varphi}^{(1)}(\boldsymbol{x})$. Critical state of the reactor is defined by the values $\alpha = 0$; when $\alpha > 0$ we get the supercritical state, and when $\alpha < 0$ — subcritical state of the reactor.

4. Numerical examples

We shall give some results of eigenvalue calculation. The elementary two-group model ($G = 2$) is used. The method of finite elements (Brenner and Scott, 2008; Quarteroni and Valli, 2008) on triangular calculation grids is used for the approximate solution of the spectral problem. The standard Lagrangian finite elements are used. The software has been developed using the engineering and scientific calculation library FEniCS (Logg et al., 2012). SLEPc has been used for numerical solution of the spectral problems. We used a Krylov-Schur algorithm with an accuracy of 10^{-15}. The following parameters were varied in the calculations:

- n — the number of triangles per one assembly (Fig. 1);
- p — the order of finite element.

We compare the calculations based on the SP$_3$ model and the diffusion model in (Avvakumov et al., 2014, 2017).
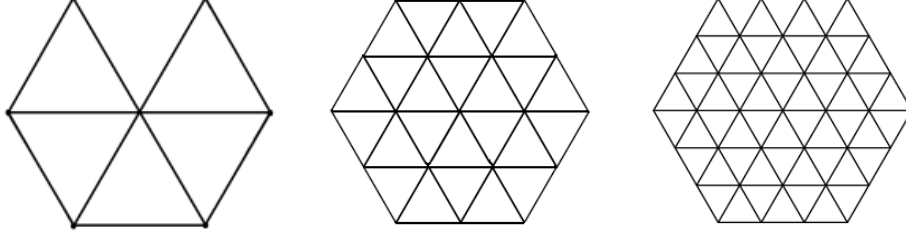

Figure 1: Discretization of assembly into 6, 24 and 96 finite elements.

4.1. IAEA-2D without reflector

The test problem for reactor IAEA-2D without reflector (Chao and Shatilla, 1995) in two-dimensional approximation (Ω is the section of reactor core) is considered. The geometrical model of the IAEA-2D reactor core consists of a set of hexagonal assemblies and is presented in Fig. 2, where the assemblies of various types are marked with various digits. The total size of assembly equals 20 cm.
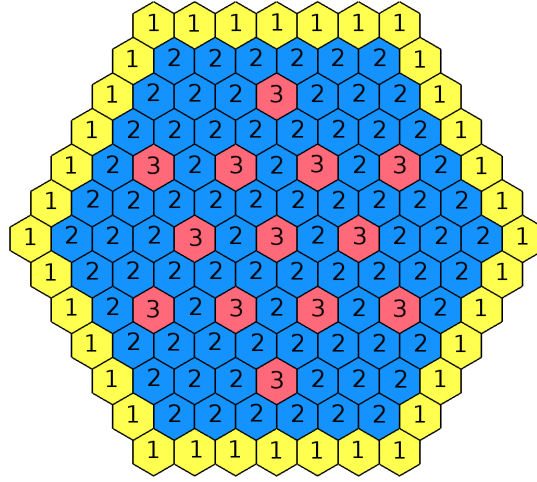

Figure 2: Geometrcial model of the IAEA-2D reactor core without reflector.

Diffusion neutronics constants in the common units are given in Table 1. The following delayed neutrons parameters are used: one group of delayed neutrons with effective fraction $\beta_1 = 6.5 \cdot 10^{-3}$ and decay constant $\lambda_1 = 0.08\,\mathrm{s}^{-1}$. Neutron velocity $v_1 = 1.25 \cdot 10^7$ cm/s and $v_2 = 2.5 \cdot 10^5$ cm/s.

Table 1: Diffusion neutronics constants for IAEA-2D.

Material	1	2	3	4
D_1	1.5	1.5	1.5	1.5
D_2	0.4	0.4	0.4	0.4
Σ_{a1}	0.01	0.01	0.01	0.0
Σ_{a2}	0.08	0.085	0.13	0.01
$\Sigma_{s,1\to2}$	0.02	0.02	0.02	0.04
$\Sigma_{s,1\to1}$	0.1922222	0.1922222	0.1922222	0.1822222
$\Sigma_{s,2\to2}$	0.7533333	0.7483333	0.7033333	0.8233333
$\nu_1\Sigma_{f1}$	0.00	0.00	0.00	0.00
$\nu_2\Sigma_{f2}$	0.135	0.135	0.135	0.00

4.1.1. Solution of Lambda Modes spectral problem

The obtained results by (Avvakumov et al., 2014) was taken as a reference solution for the diffusion model, and for the SP_3 model — the solution on a fine grid with $p = 3, n = 96$. The results of the solution of the effective multiplication factor for test IAEA-2D without a reflector are shown in table 2. Hereinafter, for λ-spectral problems, the following notation is used: k_{dif} — effective multiplication factor by diffusion model; k_{sp_3} — effective multiplication factor by SP_3 model; Δ — absolute deviation from the reference value in pcm (10^{-5}); δ — the standard deviation of the relative power.

Table 2: The effective multiplication factor.

n	p	k_{dif}	Δ_{dif}	δ_{dif}	k_{sp_3}	Δ_{sp_3}	δ_{sp_3}
	1	0.97335	473	3.80	0.97445	490	4.02
6	2	0.97760	48	0.45	0.97881	54	0.52
	3	0.97801	7	0.07	0.97925	10	0.09
	1	0.97654	154	1.28	0.97772	163	1.38
24	2	0.97799	9	0.08	0.97923	12	0.11
	3	0.97807	1	0.01	0.97934	1	0.02
	1	0.97765	43	0.36	0.97888	47	0.40
96	2	0.97807	1	0.02	0.97933	2	0.02
	3	0.97808	0	0.01	0.97935	–	–
Ref.		0.97808			0.97935		

These data demonstrate the convergence of approximate computed eigenvalues as the computational grid crowds and degree of the approximating polynomials increases — h-p finite element method. The table 3 shows the results of the first 10 eigenvalues for $p = 3, n = 96$.

The power and error distribution for $p = 2, n = 24$ is shown in the Figures 3, 4. Hereinafter, for each cassette from above, the following are given: reference

Table 3: The eigenvalues $k_i = 1/\lambda_i^{(k)}$ for $p = 3, n = 96$.

i	Diffusion	SP_3
1	$0.97808 + 0.0i$	$0.97935 + 0.0i$
2	$0.96318 + 0.0i$	$0.96460 + 0.0i$
3	$0.96318 + 0.0i$	$0.96460 + 0.0i$
4	$0.93844 + 0.0i$	$0.94025 + 0.0i$
5	$0.93844 + 0.0i$	$0.94025 + 0.0i$
6	$0.91966 + 0.0i$	$0.92184 + 0.0i$
7	$0.90220 + 0.0i$	$0.90447 + 0.0i$
8	$0.87141 + 0.0i$	$0.87500 + 0.0i$
9	$0.84957 + 0.0i$	$0.85315 + 0.0i$
10	$0.84957 + 0.0i$	$0.85315 + 0.0i$

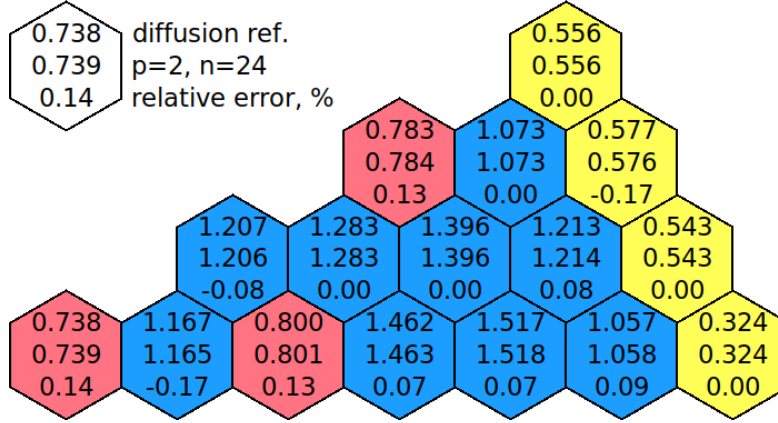solution, solution and relative error from the reference solution.

Figure 3: Power and error distributions using diffusion model.

4.1.2. Solution of Alpha Modes spectral problem

As a reference solution, the solutions obtained using the diffusion or transport model on a fine grid $p = 3, n = 96$ are taken. Hereinafter, for α-spectral problems, the following notation is used: α_{dif} — α-eigenvalue by diffusion model; α_{sp3} — α-eigenvalue by SP_3 model; Δ — absolute deviation from the reference value.

Without delayed neutrons.
With delayed neutrons.
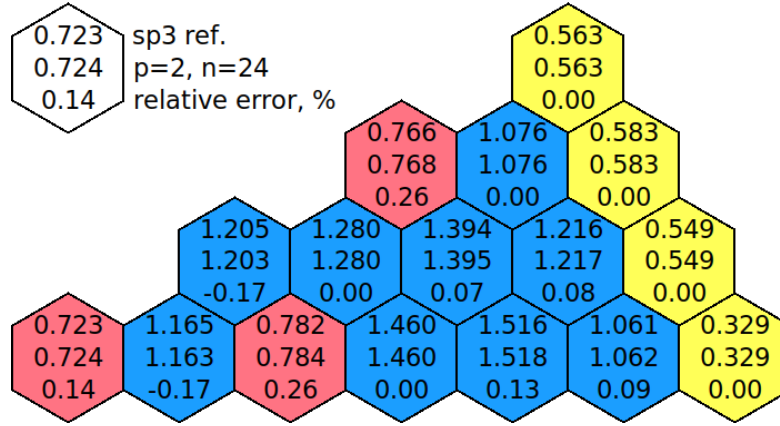
Figure 4: Power and error distributions using SP$_3$ model.

Table 4: The period eigenvalues.

n	p	α_{dif}	Δ_{dif}	α_{sp_3}	Δ_{sp_3}
	1	556.3	100.8	532.7	104.1
6	2	465.6	10.1	440.0	11.4
	3	457.0	1.5	430.7	2.1
	1	488.1	32.6	463.0	34.4
24	2	457.4	1.9	431.0	2.4
	3	455.7	0.2	428.9	0.3
	1	464.6	9.1	438.4	9.8
96	2	455.8	0.3	428.9	0.3
	3	455.5	–	428.6	–
Ref.		455.5		428.6	

4.2. IAEA-2D with reflector

Added external reflector row (material 4, see table 1).

4.2.1. Solution of Lambda Modes spectral problem

4.2.2. Solution of Alpha Modes spectral problem

As a reference solution, the solutions obtained using the diffusion or transport model on a fine grid $p = 3, n = 96$ are taken.

Without delayed neutrons.

With delayed neutrons.

4.3. Cosymmetric IAEA-2D with reflector

Two rods added. The geometrical model of reactor core is shown in Fig. 19.

Table 5: The eigenvalues $\alpha_i = \lambda_i^{(\alpha)}$ for $p = 3, n = 96$.

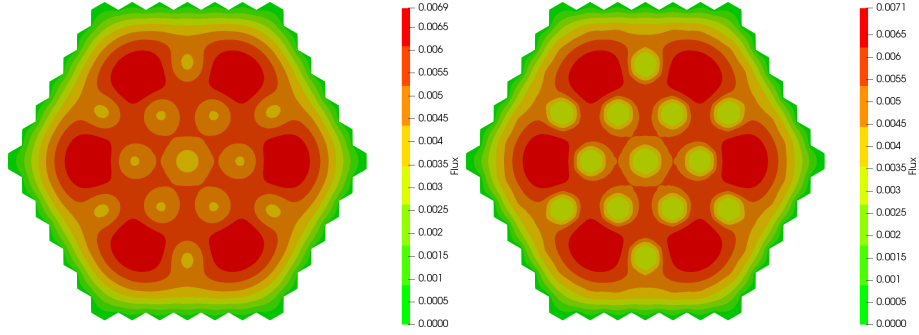| i	Diffusion	SP_3
1	$455.540 + 0.0i$	$428.561 + 0.0i$
2	$760.532 + 0.0i$	$730.398 + 0.0i$
3	$760.543 + 0.0i$	$730.408 + 0.0i$
4	$1267.192 + 0.0i$	$1228.835 + 0.0i$
5	$1267.192 + 0.0i$	$1228.836 + 0.0i$
6	$1647.145 + 0.0i$	$1601.437 + 0.0i$
7	$2083.289 + 0.0i$	$2031.778 + 0.0i$
8	$2696.887 + 0.0i$	$2616.862 + 0.0i$
9	$3188.356 + 0.0i$	$3092.715 + 0.0i$
10	$3188.363 + 0.0i$	$3092.722 + 0.0i$

Figure 5: Eigenfunctions $\phi_1^{(1)}$, $\phi_2^{(1)}$.

4.3.1. Solution of Lambda Modes spectral problem

4.3.2. Solution of Alpha Modes spectral problem

As a reference solution, the solutions obtained using the diffusion or transport model on a fine grid $p = 3, n = 96$ are taken.

Without delayed neutrons.

4.4. HWR problem

This benchmark simulate the active zone of a large heavy-water reactor HWR (Chao and Shatilla, 1995). The geometrical model of the HWR reactor core consists of a set of hexagonal assemblies and is presented in Fig. 23. The total size of assembly equals 17.78 cm. Diffusion neutronics constants in the common units are given in Table 18.
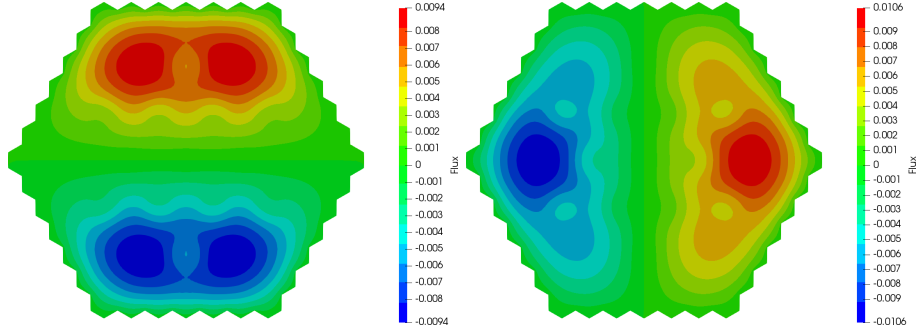
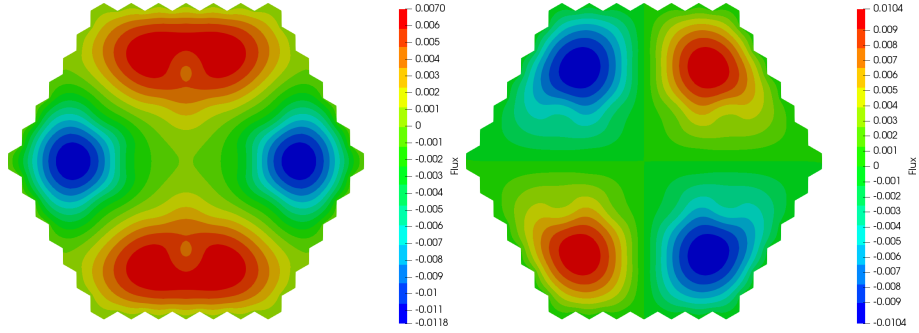Figure 6: Eigenfunctions $\phi_1^{(2)}$, $\phi_1^{(3)}$.

Figure 7: Eigenfunctions $\phi_1^{(4)}$, $\phi_1^{(5)}$.

4.4.1. Solution of Lambda Modes spectral problem

4.4.2. Solution of Alpha Modes spectral problem

As a reference solution, the solutions obtained using the diffusion or transport model on a fine grid $p = 3, n = 96$ are taken.

Without delayed neutrons.

With delayed neutrons.

Table 6: The period eigenvalues.

n	p	α_{dif}	Δ_{dif}	α_{sp_3}	Δ_{sp_3}
	1	0.06465	0.00264	0.06410	0.00295
6	2	0.06232	0.00031	0.06153	0.00035
	3	0.06206	0.00005	0.06122	0.00007
	1	0.06296	0.00095	0.06224	0.00109
24	2	0.06207	0.00005	0.06123	0.00008
	3	0.06202	0.00001	0.06116	0.00001
	1	0.06228	0.00027	0.06147	0.00032
96	2	0.06202	0.00001	0.06116	0.00001
	3	0.06201	–	0.06115	–
Ref.		0.06201		0.06115	

Table 7: The eigenvalues $\alpha_i = \lambda_i^{(\alpha)}$ for $p = 3, n = 96$.

i	Diffusion	SP$_3$
1	$0.06201 + 0.0i$	$0.06115 + 0.0i$
2	$0.06837 + 0.0i$	$0.06796 + 0.0i$
3	$0.06837 + 0.0i$	$0.06796 + 0.0i$
4	$0.07279 + 0.0i$	$0.07258 + 0.0i$
5	$0.07279 + 0.0i$	$0.07258 + 0.0i$
6	$0.07446 + 0.0i$	$0.07430 + 0.0i$
7	$0.07547 + 0.0i$	$0.07536 + 0.0i$
8	$0.07662 + 0.0i$	$0.07652 + 0.0i$
9	$0.07717 + 0.0i$	$0.07709 + 0.0i$
10	$0.07721 + 0.0i$	$0.07711 + 0.0i$

Reference

Avvakumov, A. V., Strizhov, V. F., Vabishchevich, P. N., Vasilev, A. O., 2017. Spectral properties of dynamic processes in a nuclear reactor. Annals of Nuclear Energy 99, 68–79.

Avvakumov, A. V., Vabishchevich, P. N., Vasilev, A. O., 2014. Metod konechnyh ehlementov dlya uravneniya diffuzii nejtronov v geksagonal'noj geometrii. Vestnik of North-Eastern Federal University 11 (5), 7–18.
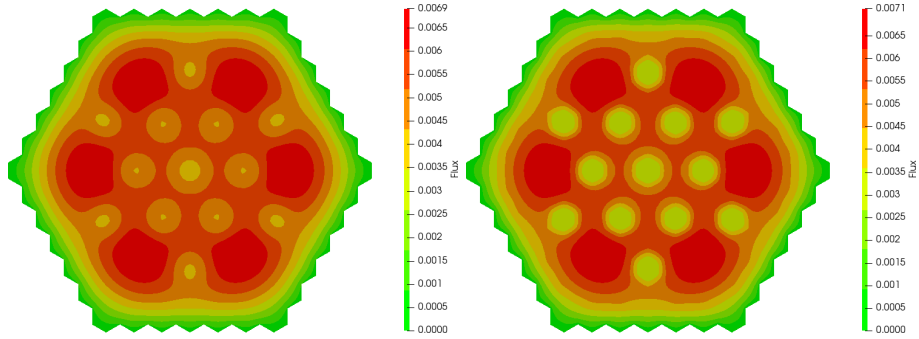
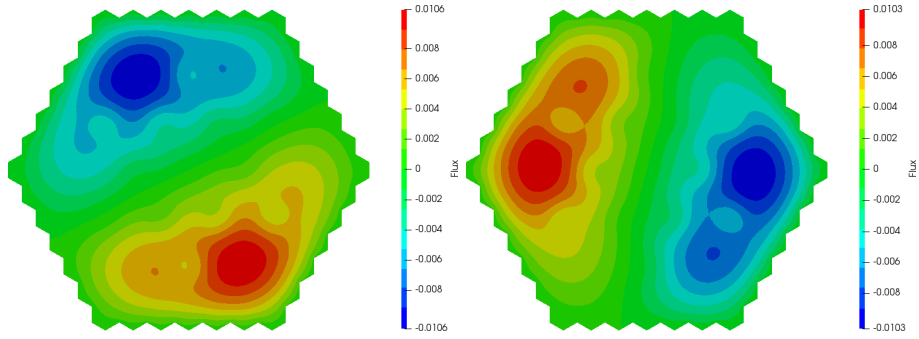Figure 8: Eigenfunctions $\phi_1^{(1)}$, $\phi_2^{(1)}$.

Figure 9: Eigenfunctions $\phi_1^{(2)}$, $\phi_1^{(3)}$.

Azmy, Y., Sartori, E., 2010. Nuclear computational science: a century in review. Springer.

Beckert, C., Grundmann, U., 2008. Development and verification of a nodal approach for solving the multigroup SP_3 equations. Annals of Nuclear Energy 35 (1), 75–86.

Bell, G. I., Glasstone, S., 1970. Nuclear Reactor Theory. Van Nostrand Reinhold Company.

Brantley, P. S., Larsen, E. W., 2000. The simplified P_3 approximation. Nuclear Science and Engineering 134 (1), 1–21.

Brenner, S. C., Scott, L. R., 2008. The mathematical theory of finite element methods. Springer.

Chao, Y. A., Shatilla, Y. A., 1995. Conformal mapping and hexagonal nodal methods-II: Implementation in the ANC-H Code. Nuclear Science and Engineering 121, 210–225.
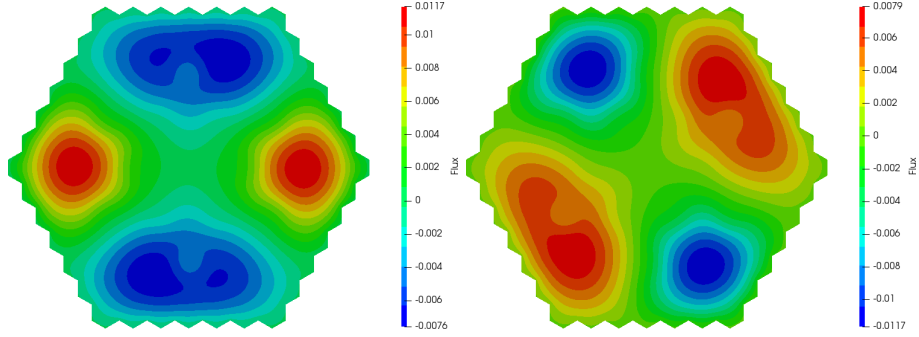
Figure 10: Eigenfunctions $\phi_1^{(4)}$, $\phi_1^{(5)}$.

Table 8: The effective multiplication factor.

n	p	k_{dif}	Δ_{dif}	δ_{dif}	k_{sp_3}	Δ_{sp_3}	δ_{sp_3}
	1	1.01041	490	13.29	1.01159	536	14.14
6	2	1.00623	72	1.88	1.00711	88	2.19
	3	1.00558	7	0.22	1.00636	13	0.35
	1	1.00699	148	4.54	1.00792	169	4.96
24	2	1.00561	10	0.30	1.00640	17	0.42
	3	1.00551	0	0.02	1.00626	3	0.17
	1	1.00591	36	1.28	1.00671	48	1.42
96	2	1.00552	1	0.04	1.00626	3	0.18
	3	1.00551	0	0.01	1.00625	2	0.18
Ref.		1.00551			1.00623		

Downar, T., Xu, Y., Seker, V., Hudson, N., 2010. Theory manual for the PARCS kinetics core simulator module. Department of Nuclear Engineering and Radiological Sciences, University of Michigan.

Gelbard, E. M., 1960. Application of spherical harmonics method to reactor problems. Bettis Atomic Power Laboratory, West Mifflin, PA, Technical Report No. WAPD-BT-20.

Gelbard, E. M., 1961. Simplified spherical harmonics equations and their use in shielding problems. Tech. rep., Westinghouse Electric Corp. Bettis Atomic Power Lab., Pittsburgh.

Gelbard, E. M., 1962. Applications of the simplified spherical harmonics equations in spherical geometry. Tech. rep., Westinghouse Electric Corp. Bettis Atomic Power Lab., Pittsburgh.

Ginestar, D., Miro, R., Verdu, G., Hennig, D., 2002. A transient modal analysis

Table 9: The eigenvalues $k_i = 1/\lambda_i^{(k)}$ for $p = 3, n = 96$.

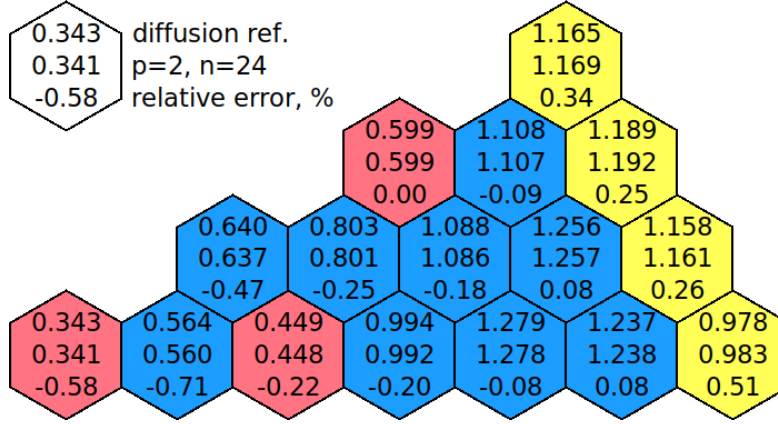| i	Diffusion	SP_3
1	$1.00551 + 0.0i$	$1.00625 + 0.0i$
2	$0.99649 + 0.0i$	$0.99725 + 0.0i$
3	$0.99649 + 0.0i$	$0.99725 + 0.0i$
4	$0.97679 + 0.0i$	$0.97776 + 0.0i$
5	$0.97679 + 0.0i$	$0.97776 + 0.0i$
6	$0.95868 + 0.0i$	$0.95990 + 0.0i$
7	$0.92898 + 0.0i$	$0.93097 + 0.0i$
8	$0.92419 + 0.0i$	$0.92593 + 0.0i$
9	$0.90479 + 0.0i$	$0.90735 + 0.0i$
10	$0.90479 + 0.0i$	$0.90735 + 0.0i$

Figure 11: Power and error distributions using diffusion model.

of a BWR instability event. Journal of Nuclear Science and Technology 39 (5), 554–563.

Lawrence, R. D., 1986. Progress in nodal methods for the solution of the neutron diffusion and transport equations. Progress in Nuclear Energy 17 (3), 271–301.

Logg, A., Mardal, K.-A., Wells, G., 2012. Automated solution of differential equations by the finite element method: The FEniCS book. Vol. 84. Springer Science & Business Media.

McClarren, R. G., 2010. Theoretical aspects of the simplified P_N equations. Transport Theory and Statistical Physics 39 (2-4), 73–109.
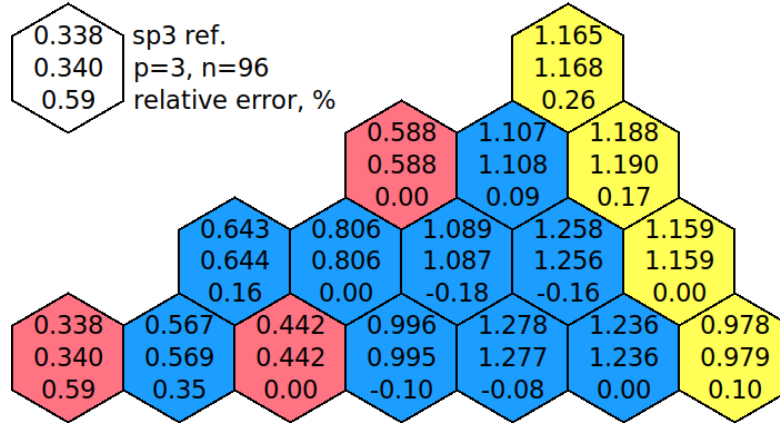
Figure 12: Power and error distributions using SP$_3$ model.

Table 10: The period eigenvalues.

n	p	α_{dif}	Δ_{dif}	α_{sp_3}	Δ_{sp_3}
	1	-184.95	84.14	-205.92	91.32
6	2	-113.58	12.77	-130.02	15.42
	3	-101.98	1.17	-116.72	2.12
	1	-126.66	25.85	-143.85	29.25
24	2	-102.58	1.77	-117.31	2.71
	3	-100.88	0.07	-114.83	0.23
	1	-107.82	7.01	-122.84	8.24
96	2	-100.97	0.16	-114.94	0.34
	3	-100.81	–	-114.60	–
Ref.		-100.81		-114.60	

Quarteroni, A., Valli, A., 2008. Numerical approximation of partial differential equations. Springer.

Ryu, E. H., Joo, H. G., 2010. Development of a 2-D simplified P$_3$ fem solver for arbitrary geometry applications.

Stacey, W. M., 2007. Nuclear Reactor Physics. Wiley.

Stewart, G. W., 2001. A Krylov–Schur algorithm for large eigenproblems. SIAM Journal on Matrix Analysis and Applications 23 (3), 601–614.

Tada, K., Yamamoto, A., Yamane, Y., Kitamuray, Y., 2008. Applicability of the diffusion and simplified P$_3$ theories for pin-by-pin geometry of BWR. Journal of nuclear science and technology 45 (10), 997–1008.

Table 11: The eigenvalues $\alpha_i = \lambda_i^{(\alpha)}$ for $p = 3, n = 96$.

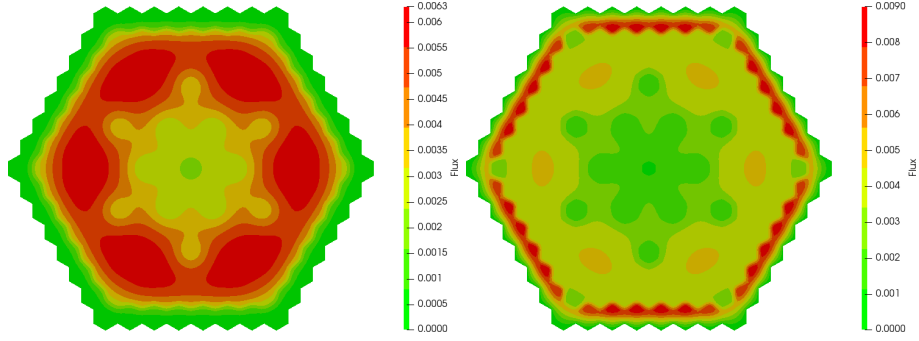| i	Diffusion	SP$_3$
1	$-100.81 + 0.0i$	$-114.60 + 0.0i$
2	$62.93 + 0.0i$	$49.42 + 0.0i$
3	$62.93 + 0.0i$	$49.42 + 0.0i$
4	$405.31 + 0.0i$	$390.15 + 0.0i$
5	$405.31 + 0.0i$	$390.15 + 0.0i$
6	$710.64 + 0.0i$	$693.47 + 0.0i$
7	$1141.43 + 0.0i$	$1118.67 + 0.0i$
8	$1469.68 + 0.0i$	$1438.31 + 0.0i$
9	$1494.37 + 0.0i$	$1468.54 + 0.0i$
10	$1494.37 + 0.0i$	$1468.54 + 0.0i$

Figure 13: Eigenfuncions $\phi_1^{(1)}$, $\phi_2^{(1)}$.

Verdú, G., Ginestar, D., 2014. Modal decomposition method for BWR stability analysis using Alpha-modes. Annals of Nuclear Energy 67, 31–40.

Verdu, G., Ginestar, D., Roman, J., Vidal, V., 2010. 3D alpha modes of a nuclear power reactor. Journal of Nuclear Science and Technology 47 (5), 501–514.
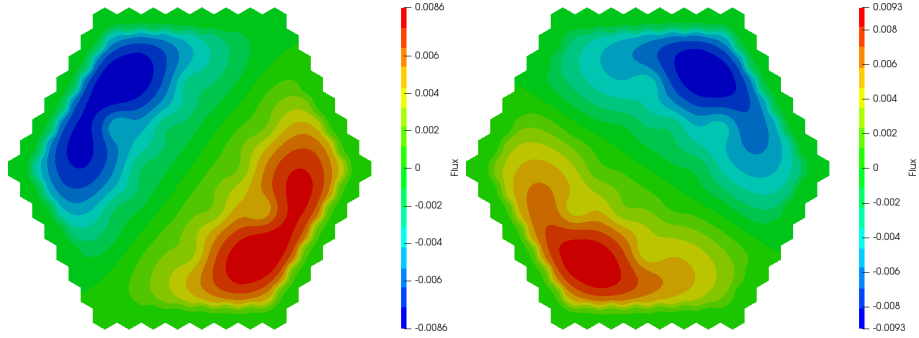
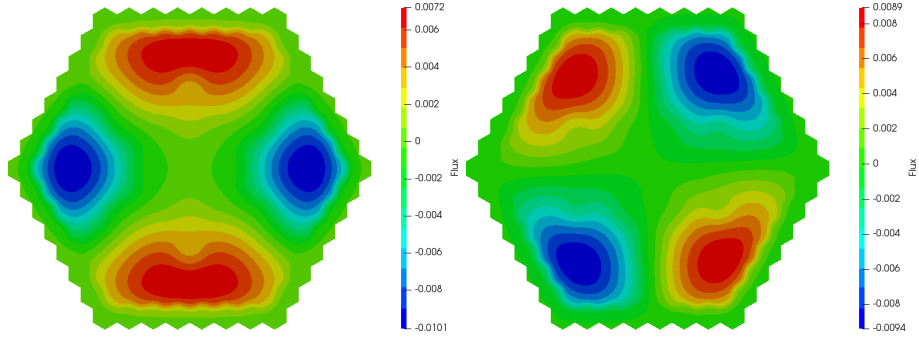Figure 14: Eigenfuncions $\phi_1^{(2)}$, $\phi_1^{(3)}$.

Figure 15: Eigenfuncions $\phi_1^{(4)}$, $\phi_1^{(5)}$.

Table 12: The period eigenvalues.

n	p	α_{dif}	Δ_{dif}	α_{sp_3}	Δ_{sp_3}
	1	-68.2268	67.8084	-88.9461	87.6086
6	2	-1.2810	0.8626	-11.1554	9.8179
	3	-0.4506	0.0322	-1.8063	0.4688
	1	-9.0267	8.6083	-25.1658	23.8283
24	2	-0.4686	0.0502	-1.9832	0.6457
	3	-0.4202	0.0018	-1.3787	0.0412
	1	-0.7018	0.2834	-4.9794	3.6419
96	2	-0.4225	0.0041	-1.3994	0.0619
	3	-0.4184	$-$	-1.3375	$-$
Ref.		-0.4184		-1.3375	

Table 13: The eigenvalues $\alpha_i = \lambda_i^{(\alpha)}$ for $p = 3, n = 96$.

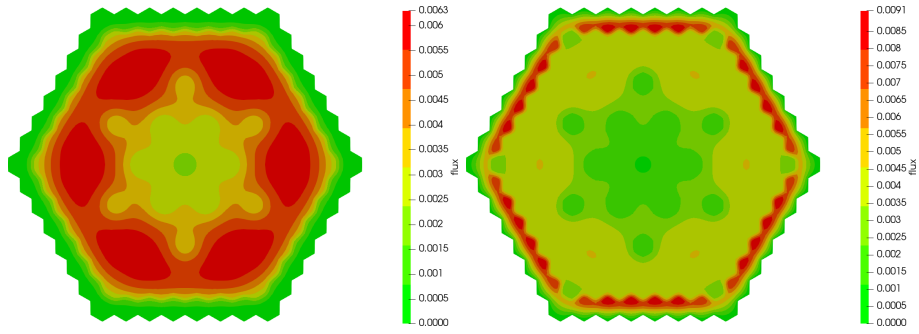| i	Diffusion	SP$_3$
1	$-0.4184 + 0.0i$	$-1.3374 + 0.0i$
2	$0.0281 + 0.0i$	$0.0238 + 0.0i$
3	$0.0281 + 0.0i$	$0.0238 + 0.0i$
4	$0.0628 + 0.0i$	$0.0622 + 0.0i$
5	$0.0628 + 0.0i$	$0.0622 + 0.0i$
6	$0.0695 + 0.0i$	$0.0692 + 0.0i$
7	$0.0737 + 0.0i$	$0.0736 + 0.0i$
8	$0.0741 + 0.0i$	$0.0740 + 0.0i$
9	$0.0754 + 0.0i$	$0.0752 + 0.0i$
10	$0.0763 + 0.0i$	$0.0762 + 0.0i$

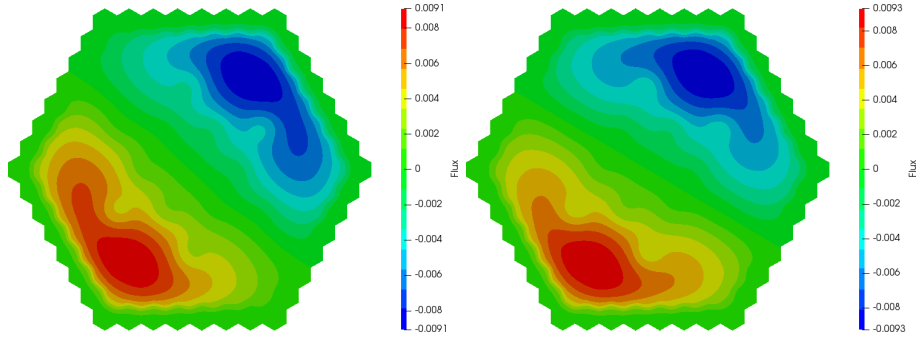Figure 16: Eigenfunctions $\phi_1^{(1)}$, $\phi_2^{(1)}$.

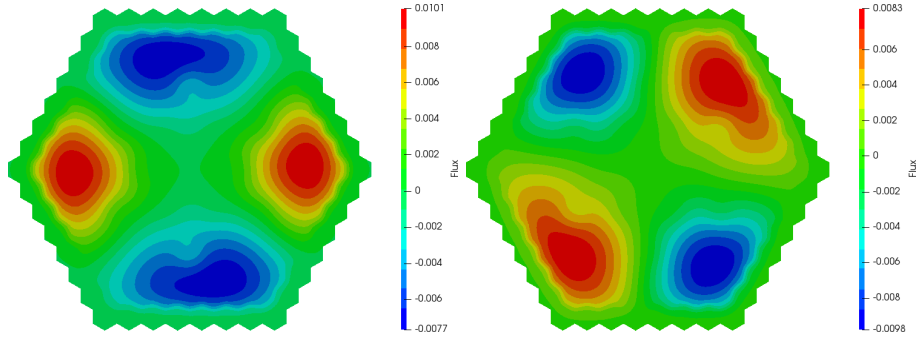Figure 17: Eigenfunctions $\phi_1^{(2)}$, $\phi_1^{(3)}$.
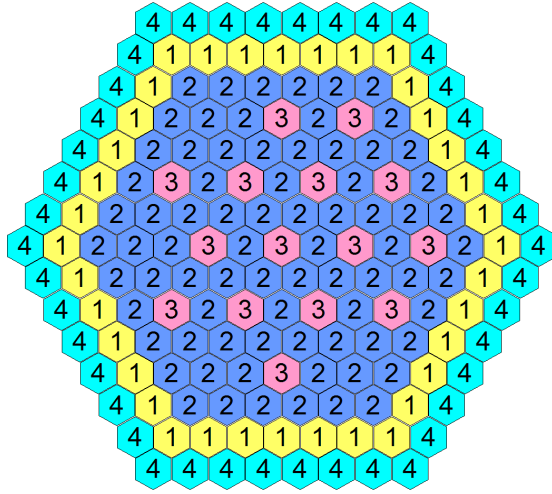
Figure 18: Eigenfunctions $\phi_1^{(4)}$, $\phi_1^{(5)}$.

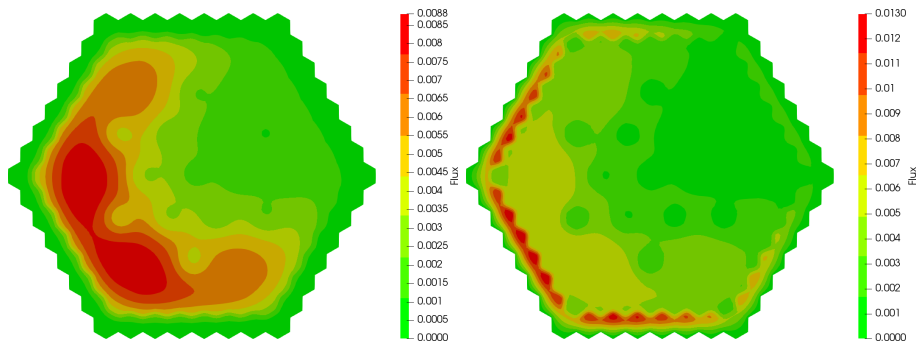Figure 19: Geometrcial model of the cosymmetric IAEA-2D reactor core with reflector.

Figure 20: Eigenfunctions $\phi_1^{(1)}$, $\phi_2^{(1)}$.

21

Table 14: The effective multiplication factor.

n	p	k_{dif}	Δ_{dif}	k_{sp_3}	Δ_{sp_3}
	1	1.00809	509	1.00931	556
6	2	1.00374	74	1.00465	90
	3	1.00306	6	1.00387	12
	1	1.00454	154	1.00550	175
24	2	1.00310	10	1.00391	16
	3	1.00300	0	1.00376	1
	1	1.00341	41	1.00424	49
96	2	1.00300	0	1.00377	2
	3	1.00300	–	1.00375	–
Ref.		1.00300		1.00375	

Table 15: The eigenvalues $k_i = 1/\lambda_i^{(k)}$ for $p = 3, n = 96$.

i	diffusion	SP$_3$
1	$1.00300 + 0.0i$	$1.00375 + 0.0i$
2	$0.99457 + 0.0i$	$0.99537 + 0.0i$
3	$0.98630 + 0.0i$	$0.98724 + 0.0i$
4	$0.97032 + 0.0i$	$0.97141 + 0.0i$
5	$0.96898 + 0.0i$	$0.97021 + 0.0i$
6	$0.94555 + 0.0i$	$0.94717 + 0.0i$
7	$0.92844 + 0.0i$	$0.93044 + 0.0i$
8	$0.92386 + 0.0i$	$0.92561 + 0.0i$
9	$0.90326 + 0.0i$	$0.90587 + 0.0i$
10	$0.90159 + 0.0i$	$0.90425 + 0.0i$

Table 16: The period eigenvalues.

n	p	α_{dif}	Δ_{dif}	α_{sp_3}	Δ_{sp_3}
	1	-143.12	88.55	-164.63	96.08
6	2	-67.99	13.42	-84.75	16.20
	3	-55.82	1.25	-70.78	2.23
	1	-81.93	27.36	-99.47	30.92
24	2	-56.45	1.88	-71.41	2.86
	3	-54.65	0.08	-68.80	0.25
	1	-62.00	7.43	-77.28	8.73
96	2	-54.74	0.17	-68.91	0.36
	3	-54.57	–	-68.55	–
Ref.		-54.57		-68.55	

Table 17: The eigenvalues $\alpha_i = \lambda_i^{(\alpha)}$ for $p = 3, n = 96$.

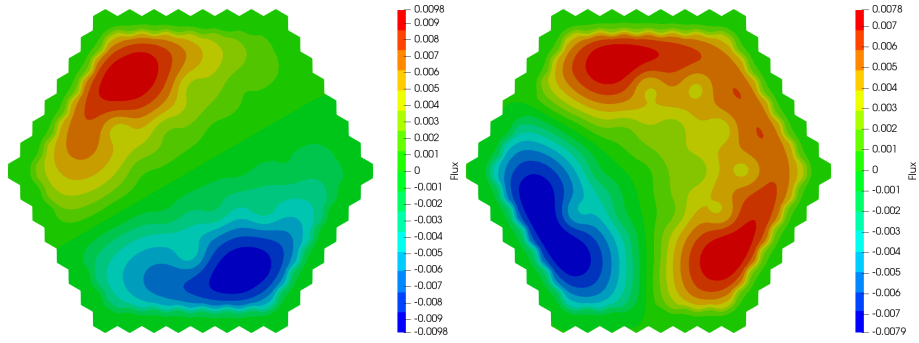| i	Diffusion	SP_3
1	$-54.57 + 0.0i$	$-68.55 + 0.0i$
2	$97.07 + 0.0i$	$83.18 + 0.0i$
3	$242.22 + 0.0i$	$226.42 + 0.0i$
4	$513.07 + 0.0i$	$496.61 + 0.0i$
5	$530.98 + 0.0i$	$512.74 + 0.0i$
6	$898.88 + 0.0i$	$878.37 + 0.0i$
7	$1148.46 + 0.0i$	$1125.66 + 0.0i$
8	$1481.13 + 0.0i$	$1449.58 + 0.0i$
9	$1512.16 + 0.0i$	$1486.05 + 0.0i$
10	$1527.83 + 0.0i$	$1501.83 + 0.0i$

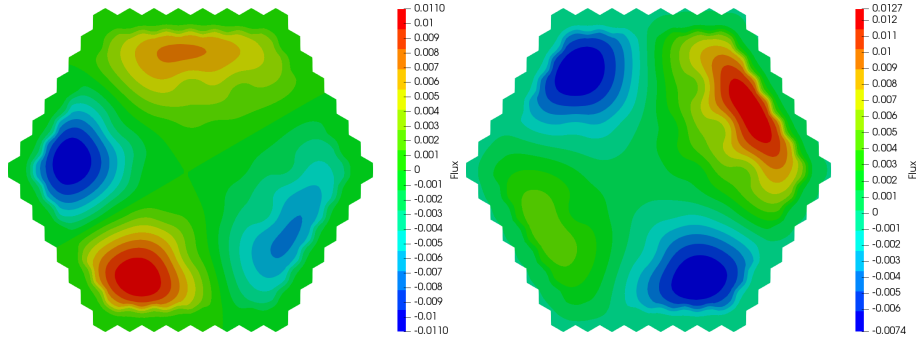Figure 21: Eigenfunctions $\phi_1^{(2)}$, $\phi_1^{(3)}$.

Figure 22: Eigenfunctions $\phi_1^{(4)}$, $\phi_1^{(5)}$.

23

Table 18: Diffusion neutronics constants for HWR.

Material	Group	D, cm	Σ_r, cm^{-1}	$\Sigma_{1\rightarrow 2}$, cm^{-1}	$\nu\Sigma_f$, cm^{-1}
1	1	1.38250058	1.1105805e-2	8.16457e-3	2.26216e-3
	2	0.89752185	2.2306487e-2		2.30623e-2
2	1	1.38255219	1.1174585e-2	8.22378e-3	2.22750e-3
	2	0.89749043	2.2387609e-2		2.26849e-2
3	1	1.37441741	1.0620368e-2	8.08816e-3	2.14281e-3
	2	0.88836771	1.6946527e-2		2.04887e-2
4	1	1.31197955	1.2687953e-2	1.23115e-2	0.0
	2	0.87991376	5.2900925e-2		0.0
6	1	1.38138909	1.056312e-2	7.76568e-3	2.39469e-3
	2	0.90367052	2.190298e-2		2.66211e-2
7	1	1.30599110	1.1731321e-2	1.10975e-2	0.0
	2	0.83725587	4.3330365e-3		0.0
8	1	1.29192957	1.1915316e-2	1.15582e-2	0.0
	2	0.81934103	3.0056488e-4		0.0
9	1	1.06509884	2.8346221e-2	2.61980e-2	0.0
	2	0.32282849	3.3348874e-2		0.0

Table 19: The effective multiplication factor.

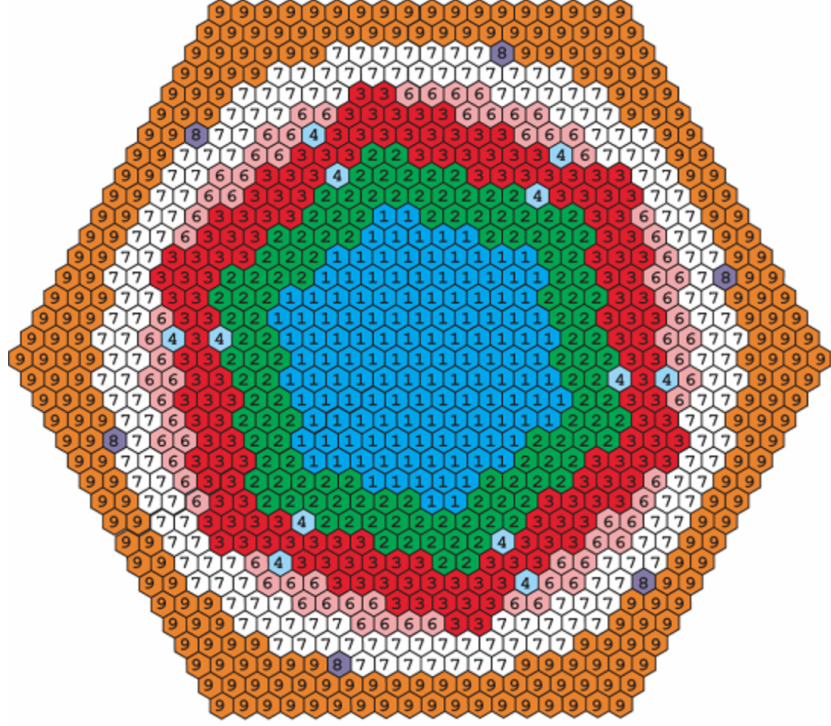| n	p	k_{dif}	Δ_{dif}	k_{sp_3}	Δ_{sp_3}
	1	0.991985	2.0	0.992178	5
6	2	0.991989	2.4	0.992166	4
	3	0.991964	0.1	0.992132	0
	1	0.991983	1.8	0.992165	3
24	2	0.991965	0.0	0.99213	0
	3	0.991963	0.2	0.99213	0
	1	0.991969	0.4	0.99214	1
96	2	0.991963	0.2	0.99213	0
	3	0.991963	0.2	0.99213	–
Ref.		0.991965		0.99213	

Figure 23: Geometrcial model of the HWR reactor core.

Table 20: The eigenvalues $k_i = 1/\lambda_i^{(k)}$ for $p = 3, n = 96$.

i	diffusion	SP_3
1	$0.99196 + 0.0i$	$0.99213 + 0.0i$
2	$0.98359 + 1.1645\text{e-}05i$	$0.98379 + 1.2072\text{e-}05i$
3	$0.98359 - 1.1645\text{e-}05i$	$0.98379 - 1.2072\text{e-}05i$
4	$0.96424 + 2.1564\text{e-}05i$	$0.96452 + 2.2337\text{e-}05i$
5	$0.96424 - 2.1564\text{e-}05i$	$0.96452 - 2.2337\text{e-}05i$
6	$0.94329 + 0.0i$	$0.94373 + 0.0i$
7	$0.92387 + 0.0i$	$0.92426 + 0.0i$
8	$0.91866 + 0.0i$	$0.91880 + 0.0i$
9	$0.89568 + 3.5570\text{e-}05i$	$0.89632 + 3.6750\text{e-}05i$
10	$0.89568 - 3.5570\text{e-}05i$	$0.89632 + 3.6750\text{e-}05i$

Table 21: The period eigenvalues.

n	p	α_{dif}	Δ_{dif}	α_{sp_3}	Δ_{sp_3}
	1	42.281	0.018	41.246	0.134
6	2	42.135	0.128	41.190	0.190
	3	42.259	0.004	41.362	0.018
	1	42.196	0.067	41.228	0.152
24	2	42.253	0.010	41.354	0.026
	3	42.263	0.000	41.379	0.001
	1	42.241	0.022	41.330	0.050
96	2	42.262	0.001	41.377	0.003
	3	42.263	–	41.380	–
Ref.		42.263		41.380	

Table 22: The eigenvalues $\alpha_i = \lambda_i^{(\alpha)}$ for $p = 3, n = 96$.

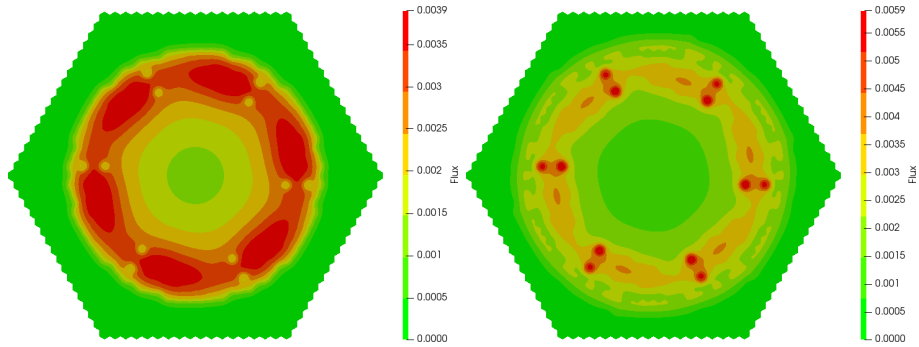| i	Diffusion	SP$_3$
1	$42.263 + 0.0i$	$41.380 + 0.0i$
2	$84.867 - 0.06130i$	$83.821 - 0.06358i$
3	$84.867 + 0.06130i$	$83.821 + 0.06358i$
4	$182.914 - 0.11367i$	$181.471 - 0.11805i$
5	$182.914 + 0.11367i$	$181.471 + 0.11805i$
6	$293.017 + 0.0i$	$290.940 + 0.0i$
7	$371.528 + 0.0i$	$369.374 + 0.0i$
8	$515.465 - 0.16397i$	$512.337 - 0.17197i$
9	$515.465 + 0.16397i$	$512.337 + 0.17197i$
10	$518.670 + 0.0i$	$517.975 + 0.0i$

Figure 24: The eigenfunctions $\phi_1^{(1)}$ (left) and $\phi_2^{(1)}$ (right).
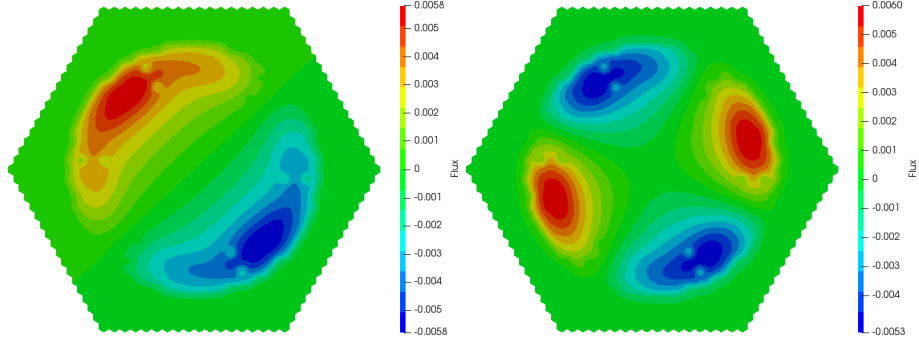
Figure 25: Real part of eigenfunctions $\phi_1^{(2)}$, $\phi_1^{(3)}$ (left) and $\phi_1^{(4)}$, $\phi_1^{(5)}$ (right).
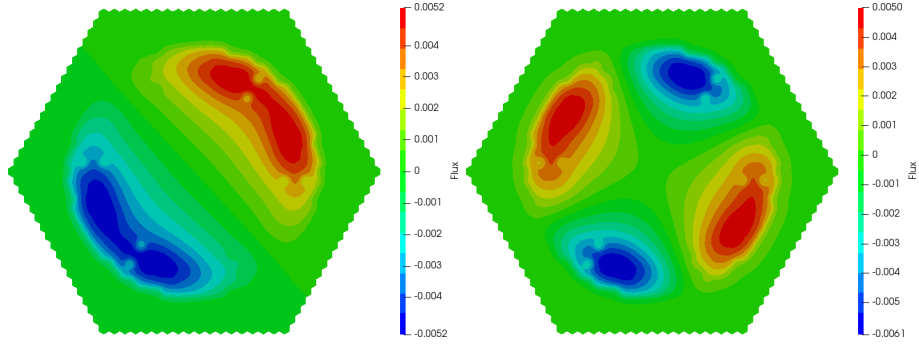

Figure 26: Imaginary part of eigenfunctions $\phi_1^{(2)}$, $-\phi_1^{(3)}$ (left) and $\phi_1^{(4)}$, $-\phi_1^{(5)}$ (right).

Table 23: The period eigenvalues.

n	p	α_{dif}	Δ_{dif}	α_{sp_3}	Δ_{sp_3}
	1	0.04431	0.	0.04383	0.
6	2	0.04430	0.	0.04386	0.
	3	0.04437	0.	0.04394	0.
	1	0.04432	0.	0.04386	0.
24	2	0.04436	0.	0.04394	0.
	3	0.04437	0.	0.04395	0.
	1	0.04435	0.	0.04392	0.
96	2	0.04437	0.	0.04395	0.
	3	0.04437	–	0.04395	–
Ref.		–		–	

27

Table 24: The eigenvalues $\alpha_i = \lambda_i^{(\alpha)}$ for $p = 3, n = 96$.

i	Diffusion	SP_3
1	$0.04437 + 0.0i$	$0.04395 + 0.0i$
2	$0.05755 - 1.15549\text{e-}05i$	$0.05735 - 1.22333\text{e-}05i$
3	$0.05755 + 1.15549\text{e-}05i$	$0.05735 + 1.22333\text{e-}05i$
4	$0.06807 - 6.35264\text{e-}06i$	$0.06798 - 6.66947\text{e-}06i$
5	$0.06807 + 6.35264\text{e-}06i$	$0.06798 + 6.66947\text{e-}06i$
6	$0.07219 + 0.0i$	$0.07213 + 0.0i$
7	$0.07415 + 0.0i$	$0.07412 + 0.0i$
8	$0.07453 + 0.0i$	$0.07452 + 0.0i$
9	$0.07577 - 1.52484\text{e-}06i$	$0.07574 - 1.60360\text{e-}06i$
10	$0.07577 + 1.52484\text{e-}06i$	$0.07574 + 1.60360\text{e-}06i$